SBCC 2025
II Simpósio Brasileiro de Ciência do Cimento

HYDRATION KINETICS OF LOW CARBON CEMENT FROM RECYCLED ASBESTOS-CEMENT WASTE

Cinética De Hidratação de Cimento Circular de Baixo Carbono Produzido Com Resíduo de Cimento-Amianto Tratado Termicamente

Gessivaldo Oliveira Carneiro
Federal University of Bahia | Salvador, Bahia | gessivaldo19@outlook.com

Vanderley M John
University of São Paulo | São Paulo, São Paulo | vmjohn@usp.br

Cleber Marcos Ribeiro Dias
Federal University of Bahia | Salvador, Bahia | clebermrd@gmail.com

ABSTRACT

This study aims to evaluate the hydration kinetics of circular low-carbon cement (C²BC) obtained from the heat treatment of asbestos cement waste raw (ACW_{nat}). The research aims to understand the hydration mechanism of C²BC by comparing it with Portland cement. To this end, this study analyzed C²BC pastes, and CPII-F 32 as a reference, with a water/solid mass ratio of 0.60. The pastes were analyzed using isothermal calorimetry, in situ XRD, chemically combining water and compressive strength. The results indicated that the C²BC pastes had lower hydration rates, accumulated heat, and combined water content up to 28 days than the reference pastes, but higher compressive strength, attributed to the refinement of the microstructure defects in the C²BC pastes. It was possible to validate the formation of ettringite and C-S-H in the early stages of hydration of C²BC, and the depletion of sulfates in CPII-F 32. C²BC has the potential to be used as a low environmental impact binder.

Keywords: Asbestos cement waste; thermal treatment; CO_2 emissions; low-carbon circular cement.

1 INTRODUCTION

Asbestos fibers were widely used as reinforcement in cement artifacts due to their physical and chemical properties (BLOISE; CATALANO; GUALTIERI, 2018), especially in asbestos-cement tiles (BIANCHI; BIANCHI, 2015). With the discovery of the carcinogenic potential of these fibers, more than 75 countries, including Brazil in 2017, banned their exploitation (STAYNER; WELCH; LEMEN, 2013). According to (SPASIANO; PIROZZI, 2017), between 1900 and 2015, approximately 210 million tons of asbestos fibers were traded worldwide, resulting in the production of more than 2.4 billion tons of manufactured goods containing asbestos. In Brazil, during the same period, the industrialization of 8.8 million tons of chrysotile asbestos generated approximately 100 million tons of artifacts (CARNEIRO et al., 2021).

Therefore, the search for sustainable alternatives for the disposal of asbestos-cement waste (ACW) and/or eliminating its carcinogenic liabilities has become a priority. Reverse logistics stands out as the main strategy for focusing on optimizing treatment methods and the use of inert waste. Carneiro et al. (2021) proposed an innovative and sustainable solution to optimize thermal treatment, establishing ideal conditions for the complete dehydroxylation of asbestos, minimizing CO_2 emissions and energy consumption, in addition to maximizing the crystallization of the dicalcium silicate polymorph (α'_H-C_2S), giving the treated waste an agglomerating character. In this sense, strategies that promote the development of low-carbon circular binders, including inertized ACW, can enhance the mitigation of the environmental footprint generated by the cement industry. However, studies aimed at understanding the hydration kinetics involving C²BC are still in their infancy.

This study investigates the hydration mechanisms of C²BC produced from the heat treatment of ACW_{nat}, evaluating its potential as an alternative hydraulic binder. For this purpose, the heat flux, accumulated heat, chemically combined water content, and mineralogical composition were analyzed, using in situ XRD in C²BC pastes. In addition, the compressive strengths of the paste were evaluated over time and compared with those of Portland cement CPII-F 32, used as a reference.

2 METHODOLOGY

2.1 MATERIALS

The experimental study used heat-treated asbestos cement waste (ACW_T) according to the methodology proposed by Carneiro et al. (2021), known in this study as low-carbon circular cement (C^2BC), and Portland cement. C^2BC had a specific mass of 3.05 g/cm³, determined in a Micromeritics AccuPyc II-1340 helium gas pycnometer, and a specific BET surface area of 10.70 m²/g. Portland cement with limestone filler (CPII-F 32), similar to the European cement CEM II 40 of standard EN 197-1, had a specific mass of 3.15 g/cm³ and a BET of 1.25 m²/g. The chemical composition of C^2BC and CPII-F 32 was obtained utilizing X-ray fluorescence (XRF). They differ mainly in their SiO_2 and MgO contents, which are higher for C^2BC, as they partially originate from the asbestos fibers present in ACW_{nat}. The crystalline phases present in the asbestos cement waste raw (ACW_{nat}) and in the C^2BC were determined by Carneiro et al. (2021), with C^2BC, the dicalcium silicate polymorph (α'_H-C_2S) and calcite as the majority phases, with an amorphous content of 40%.

2.2 METHODS FOR ANALYZING THE HYDRATION KINETICS OF THE MIXTURE

To evaluate the hydration mechanisms of C^2BC and CPII-F 32, a fixed water/cement ratio of 0.60 (by mass) was used, allowing C^2BC to be molded. The mixtures were produced from the following steps: i) addition of water to the powder for 5 s; ii) manual mixing with a spatula for 25 s; and iii) mechanical dispersion in a mixer at 1000 rpm for 30 s. An isothermal calorimeter, model Calmetrix I-CAL 8000 HPC, was used to analyze the heat flow and accumulated heat at 23 °C for 168 h. To analyze the chemically bound water, a Netzsch T209 F1 Libra thermobalance was used in an inert atmosphere (N2), with approximately 50 mg in an open alumina crucible and heated at a rate of 20 °C/min, based on the method proposed by (ABRÃO; CARDOSO; JOHN, 2019). To complement the reaction kinetics analysis, in situ X-ray diffraction was used using an Empyrean diffractometer (Panalytical), equipped with a PIXcel3D detector, operating with (CuKα), and radiation of 40 kV and 40 mA, from 7-70° about 2θ and with a step of 0.02°. The mixture was added to the sample holder and covered with a Kapton polymer film, performing the analysis every 10 min and at 20 min intervals for 48 h. The compressive strength of the pastes in cubic specimens with 20 mm edges, cured in a humid chamber at 23 ± 2 °C and relative humidity ≥ 95%, were analyzed after 1, 3, and 7 days of curing, using an Instron universal press, model 5569, with a 50 kN load cell, and displacement speed equal to 0.30 mm/min.

3 RESULTS AND DISCUSSION

3.1 CALORIMETRIC ANALYSIS

The curves in Figure 1a show that the maximum heat flow of C^2BC was approximately 43% higher than that of CPII-F 32 in the first 4 hours, explained by the high surface area, instability of the dehydrated products, the amorphous content, and the CaO hydration reaction. This effect can be observed in thermoactivated recycled cements (RC) by Shui et al. (2009) and Wang, Mu and Liu (2018). For Angulo et al. (2022), more than 50% of the accumulated heat is related to reactions involving CaO in cement fines obtained from construction and demolition waste (CDW) calcined at 650 °C. For the CPII-F 32 paste, the heat rate is related to the wetting of the particles and the initial dissolution of C_3A and C_3S and alkaline sulfates (SCRIVENER et al., 2023). On the other hand, the induction, acceleration, and deceleration stages inherent in the two systems reflected different behaviors due to the variation in the hydraulic phases present. According to Juilland et al. (2010), among the theories that explain the induction period in cementitious mixtures, the dissolution of C_3S, associated with crystallographic defects and saturation of the solution, is the most plausible explanation for this phenomenon. For CPII-F 32, the end of induction occurred in 4.52 h, thus validating the understanding of the dissolution of C_3S, while for C^2BC, in 12.93 h, as it does not have C_3S and C_3A, this may be associated with the dissolution of α'_H-C_2S, and the degree of rehydration of C-S-H and ettringite in the initial reactions.

Figure 1b1 shows the acceleration period of the paste with CPII-F 32, which is related to the effects of nucleation and precipitation of C-S-H with the simultaneous formation of portlandite (JUILLAND et al., 2010), after supersaturation of the solution with calcium, which generated a maximum heat flow equal to 3.40 mW/g of cement. However, in Figure 1b2, the α'_H-C_2S polymorph may have contributed to heat release after 12.93 h, forming portlandite and C-S-H with a lower Ca/Si ratio compared to the CPII-F 32 paste. Although α'_H-C_2S is the most reactive of the dicalcium silicates, the heat flow was around 6 times lower, due to its lower solubility compared to C_3S, and the difference in the amount of these phases in the two systems.

Figure 1 also shows that the heat accumulated over 7 days for CPII-F 32 was 2 times greater than that of C^2BC, corresponding to ~50% of the total heat of CPII-F 32, in line with (ANGULO et al., 2022). On the other

hand, the initial reaction of C²BC was faster than that of CPII-F 32, reflecting a greater accumulated heat in the first 9 hours of hydration. This phenomenon can be explained, in part, by the greater reactivity of α'$_H$-C_2S compared to β-C_2S (SERPELL; ZUNINO, 2017), and the reformation of calcium silicate hydrated and ettringite (ANGULO et al., 2022).

Figure 1 - Isothermal calorimetry analysis of CPII-F 32 and C²BC, in which a) heat flow and heat during 2 h of reaction, b1) heat flow and its second derivative over time, indicating the start of portlandite formation at ~13 hours, and b2) sulfate depletion at ~17 hours.

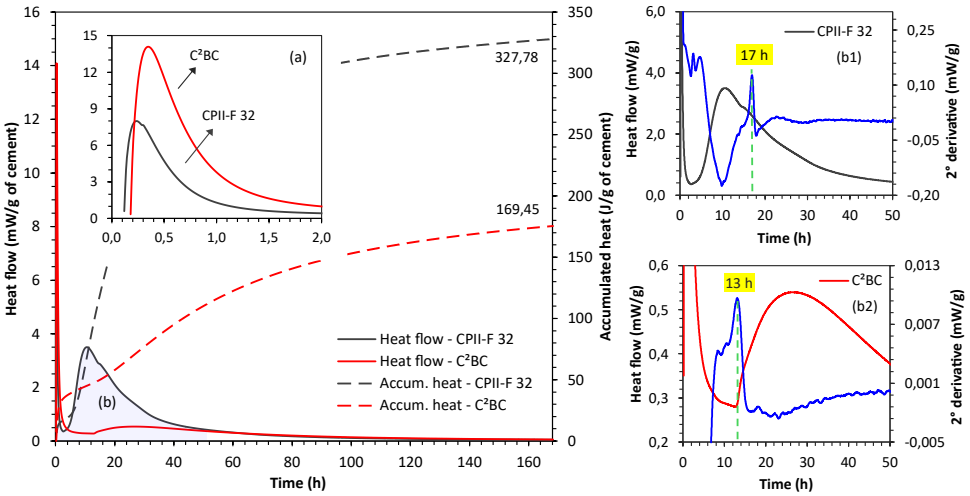

3.3 COMPRESSIVE STRENGTH VERSUS COMBINED WATER

The CPII-F 32 and C²BC mixtures showed similar results at 1 and 3 days of hydration, but after 7 days, the C²BC paste had a 20% higher strength than CPII-F 32 for the same w/c ratio. This effect, described by Serpell and Zunino (2017), can be explained by the depolymerization of C-S-H and the crystallization of the highly reactive α'$_H$-C_2S polymorph, after heat treatment of ACW_{nat} at 800 °C. In addition, the reformation of C-S-H and ettringite (ANGULO et al., 2022) may have contributed to the increase in compressive strength. Figure 2b shows that C²BC required ~3% less combined water to reach the strength than CPII-F 32, possibly due to the smaller size of defects or greater volume of solids with the same combined water. Figure 2 shows a 50% reduction in the accumulated heat of the C²BC paste at 7 days compared to CPII-F 32, which, together with the higher compressive strength, can be attributed to the refinement of the microstructure and the absence of C_3S and C_3A in C²BC. There was also a strong correlation between compressive strength and accumulated heat in the CPII-F 32 and C²BC mixtures.

Figure 2 - Compressive strength versus chemically combined water and accumulated heat.

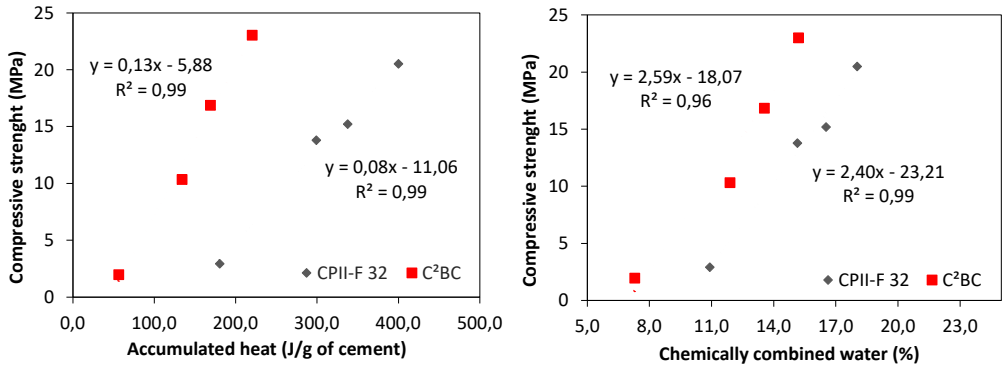

3.3 XRD IN SITU

Figure 3a shows the X-ray diffractograms of the pastes with C²BC for 48 h. In Figure 3a1, the precipitation of ettringite (9.14°, 15.86°, and 32.42°, 2θ) is observed in the first 10 min of contact of C²BC with deionized water, favored by the presence of amorphous alkaline sulfates and low-solubility anhydrite present in the anhydrous C²BC. In Figure 3b1, referring to the CP II F-32 paste, the precipitation of ettringite is observed as the gypsum is dissolved, releasing sulfate ions. Sulfate depletion occurs after ~17 h, in agreement with the 2° derivative of the heat flux (see Figure 1b1). In contrast to CPII-F 32, during the first 30 min, it was not possible to identify the formation of ettringite, which can be explained by the low degree of supersaturation (POUPELLOZ; GAUFFINET; NONAT, 2020). On the other hand, the precipitation of portlandite (CH) in the mixture with CPII-F 32 (see Figure 3b2) began around ~6 h, at the end of the induction period, reflecting a

solution supersaturated with calcium ions. With this, the nucleation and precipitation of C-S-H began on the surface of the C_3S grains, with the precipitation of CH occurring simultaneously (JUILLAND et al., 2010). In the C²BC pastes, portlandite precipitation began at around 13 hours, according to the second derivative of the heat flow (see Figure 1b1), in which the longer induction period may be related to the lower solubility of the α'_H-C_2S polymorph about C_3S. The dissolution of the silicates and/or aluminates around 31.5° to 34° 2θ led to a reduction in the peaks associated with the formation of hydrated compounds as a function of time. The formation of hydrotalcite [$Mg_6Al_2(OH)_{18}.3(H_2O)$] in the C²BC is also noted, associated with the replacement of Mg^{2+} ions by Al^{3+} and Fe^{3+}, with a peak centered at 11.20° 2θ.

Figure 3 - Illustration of the diffractograms obtained by in situ XRD of a) C²BC and b) CPII-F 32, highlighting the main events in the formation and consumption of crystalline phases.

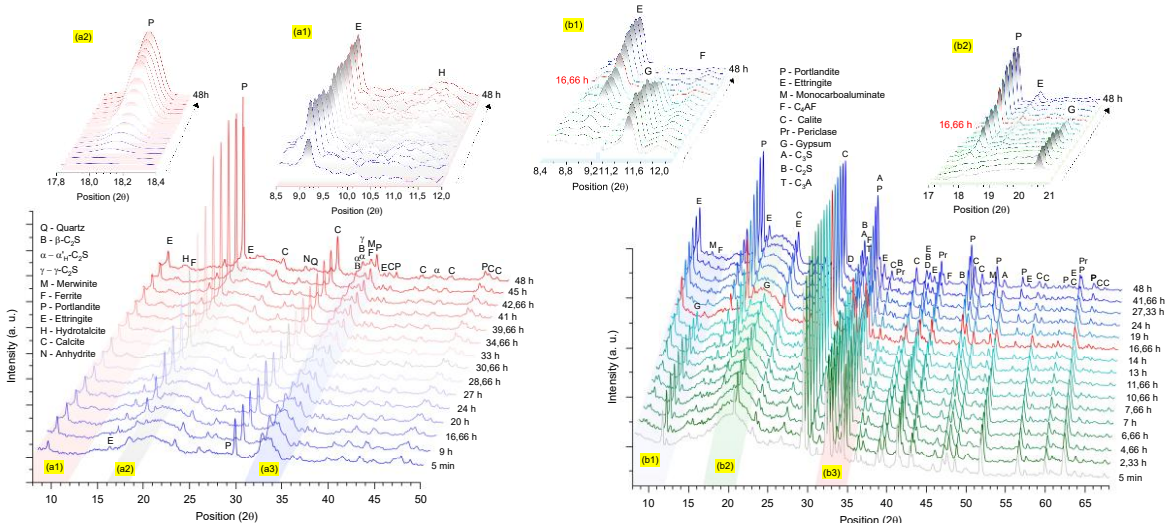

4 CONCLUSIONS

The low carbon circular cement (C²BC), obtained by the heat treatment of ACW_{nat}, presented a different hydration kinetics from CPII-F 32, as evidenced by the analysis of the heat rate and accumulated heat. In situ, XRD and the 2nd derivative of the heat rate identified the depletion of sulfates in the mixture with CPII-F 32 and the precipitation of portlandite in both systems. The C-S-H of C²BC precipitated in the early stages, together with ettringite, differing from CPII-F 32. With half the accumulated heat, C²BC showed superior mechanical performance, lower chemically combined water content, and microstructure with fewer defects. Although the rheological behavior still needs to be investigated, C²BC showed promise as an alternative to CPII-F 32.

5 ACKNOWLEDGEMENTS

The authors would like to thank the National Council for Scientific and Technological Development (CNPq) for its financial support, through process no. 404262/2023-6, and the Microstructure and Eco-efficiency Laboratory (LME-USP) for providing the necessary infrastructure to carry out this research.

BIBLIOGRAPHY

ABRÃO, P. C. R. A.; CARDOSO, F. A.; JOHN, V. M. Evaluation of Portland pozzolan blended cements containing diatomaceous earth. **Cerâmica**, v. 65, p. 75–86, 2019.

ABRÃO, P. C. R. A.; CARDOSO, F. A.; JOHN, V. M. Efficiency of Portland-pozzolana cements: Water demand, chemical reactivity and environmental impact**. Construction and Building Materials**, v. 247, 2020.

ANGULO, S. C.; GUILGE, M. S.; QUARCIONI, V. A.; CINCOTTO, M. A.; NOBRE, T. R. S.; PÖLLMANN, H. The role of calcium silicates and quicklime on the reactivity of rehydrated cements. **Construction and Building Materials**, v. 340, p. 127625, 2022.

BIANCHI, C.; BIANCHI, T. Asbestos between science and myth. A 6,000-year story. **Medicina del Lavoro**, v. 106, n. 2, p. 83–90, 2015.

BLOISE, A.; CATALANO, M.; GUALTIERI, A. F. Effect of grinding on chrysotile, amosite and crocidolite and implications for thermal treatment. **Minerals**, v. 8, n. 4, 2018.

CARNEIRO, G. O.; SANTOS, T. A.; SIMONELLI, G.; RIBEIRO, D. V.; CILLA, M. S.; DIAS, C. M. R. Thermal treatment optimization of asbestos cement waste (ACW) potentializing its use as alternative binder. **Journal of Cleaner Production**, v. 320, 2021.

JUILLAND, P.; GALLUCCI, E.; FLATT, R.; SCRIVENER, K. Dissolution theory applied to the induction period in alite hydration. **Cement and Concrete Research**, v. 40, n. 6, p. 831–844, 2010.

POUPELLOZ, E.; GAUFFINET, S.; NONAT, A. Study of nucleation and growth processes of ettringite in diluted conditions. **Cement and Concrete Research**, v. 127, p. 105915, 2020.

SCRIVENER, K. L.; JOHN, V. M.; GARTNER, E. Eco-efficient cements: Potential economically viable solutions for a low-CO_2 cement-based materials industry. **Cement and Concrete Research**, v. 114, p. 2–26, 2018.

SCRIVENER, K. L.; MATSCHEI, T.; GEORGET, F.; JUILLAND, P.; MOHAMED, A. K. Advances in hydration and thermodynamics of cementitious systems. **Cement and Concrete Research**, v. 174, p. 107332, 2023.

SERPELL, R.; ZUNINO, F. Recycling of hydrated cement pastes by synthesis of α'_H-C_2S. **Cement and Concrete Research**, v. 100, p. 398–412, 2017.

SHUI, Z.; XUAN, D.; CHEN, W.; YU, R.; ZHANG, R. Cementitious characteristics of hydrated cement paste subjected to various dehydration temperatures. **Construction and Building Materials**, v. 23, n. 1, p. 531–537, 2009.

SPASIANO, D.; PIROZZI, F. Treatments of asbestos containing wastes. **Journal of Environmental Management**, v. 204, p. 82–91, 2017.

STAYNER, L.; WELCH, L. S.; LEMEN, Richard. The Worldwide Pandemic of Asbestos-Related Diseases. **Annual Review of Public Health**, p. 205–2016, 2013.

WANG, J.; MU, M.; LIU, Y. Recycled cement. **Construction and Building Materials**, v. 190, p. 1124–1132, 2018.